Am J Transl Res 2017;9(2):580-590
www.ajtr.org /ISSN:1943-8141/AJTR0037958

Original Article

Preclinical and clinical evaluation of the liver tumor irreversible electroporation by magnetic resonance imaging

Matteo Figini[1], Xifu Wang[1], Tianchu Lyu[1], Zhanliang Su[1], Daniele Procissi[1], Vahid Yaghmai[1,2], Andrew C Larson[1,2], Zhuoli Zhang[1,2]

[1]Department of Radiology, Feinberg School of Medicine, Northwestern University, Chicago, IL, USA; [2]Robert H. Lurie Comprehensive Cancer Center, Northwestern University, Chicago, IL 60611, USA

Received August 15, 2016; Accepted November 2, 2016; Epub February 15, 2017; Published February 28, 2017

Abstract: Irreversible electroporation (IRE) is a relatively new technique for tumor ablation. It has shown promising results in difficult cases where surgery is not recommended and delicate anatomic structures are present near or within the tumor. Currently, liver cancer is one of the most common targets for IRE treatment. Pre-operative and post-operative imaging has a key role in IRE procedures and research studies. Although ultrasound is usually the first choice, especially for intra-operative guidance, magnetic resonance imaging (MRI) plays an important role in the visualization and characterization of tumor before and after IRE in clinical and preclinical studies. However, the appearance of liver lesions after IRE with different MRI sequences has never been systematically investigated, and the most common practice is to limit the acquisition protocol to only contrast-enhanced T1-weighted images. In this work, the role of MRI in clinical and preclinical assessment of hepatic tumors treated with IRE is reviewed and discussed.

Keywords: Irreversible electroporation, liver, magnetic resonance imaging, therapy response

Introduction

Electroporation is the use of an electric field to create nanopores in cell membranes, thus making them more permeable. This permeabilization can be temporary or permanent depending on the amplitude and duration of the applied electric field, and the corresponding procedures are consequently called reversible (RE) and irreversible (IRE) electroporation. Although IRE has been studied for many years, it has been applied to cancer treatment only relatively recently [1]. Many studies have demonstrated the feasibility and safety of IRE [2-7]. Compared to other techniques for tumor ablation, such as cryosurgery, focused ultrasound, interstitial laser coagulation and radiofrequency ablation, IRE has the advantage that the created ablation zone is well demarcated; its extent can be accurately controlled; and it can be obtained with an easy and short procedure. It also avoids the adverse effects related to the use of high temperatures. In particular, it preserves vital structures within and in proximity to the treated area, such as blood vessels [8]. IRE is increasingly being used for tumor treatment in patients who are not surgical candidates. The liver is an ideal target organ, due to its sensitivity to thermal damage and the presence of delicate anatomic structures such as hepatic vessels and bile ducts [9]. The preservation of these structures after IRE has been confirmed by many studies by many studies [10-12].

Imaging techniques have a key role in IRE studies. Pre-operatively, images are acquired to characterize the tumor, in particular its location and dimension, to plan the treatment in terms of the number and arrangement of electrodes and the parameters of the electric pulses. Imaging is also used during the intervention to guide electrode placement. In the immediate post-operative period imaging is used to verify that ablation is performed as planned and to check for the occurrence of acute complications. At later time points, imaging is essential

for monitoring of the treated area to better understand the evolution of the lesion and the involved biological processes, and in particular to verify the response to treatment and possibly to plan further therapeutic interventions.

Ultrasound (US) is the most frequently used modality and the only one that can be applied during the treatment with IRE. Computed Tomography (CT) is commonly used pre- and post therapy due to its availability. However, magnetic resonance imaging (MRI) scanning has distinct advantages over US and CT due to its excellent soft tissue contrast and its ability to provide dynamic contrast enhancement data.

In the following sections, published clinical and preclinical studies applying MRI before and/or after liver IRE are reviewed.

Clinical studies

The primary purpose of most of the clinical studies on liver IRE that have included MRI examinations is to assess the feasibility and the effects of the treatment, rather than to evaluate the performance of MRI sequences in the visualization of biophysical changes after IRE. The only goal of imaging of the treated area is to search for the presence of residual viable tumor and to inspect the surrounding area for complications, in particular when the ablated tumor is close to important structures such as vessels or bile ducts.

The acquisition protocol for tumor assessment before or after IRE typically includes contrast-enhanced T1-weighted MRI that is performed after the injection of a gadolinium-based contrast agent. The time between the contrast injection and scanning has to be taken into account because contrast enhancement has different phases (hepatic arterial, portal venous, equilibrium, delayed, and hepatobiliary excretion [13]), so the right timing has to be chosen to focus on specific structures and tumor. For example, when assessing hepatocellular carcinoma, arterial and venous phases are mandatory. In colorectal cancer liver metastases, arterial phase is less important.

Sometimes T2-weighted and diffusion-weighted images are acquired in liver IRE patients, but they are less common than contrast-enhanced T1-weighted imaging as their roles in the assessment of response to IRE therapy is not widely established. Quantitative MRI analyses have been performed only sporadically. See **Table 1** for a summary of the clinical studies, including a brief description of the acquisition protocol and of the quantitative analyses that were performed, if any.

MRI assessment of response to treatment

The main purpose of clinical studies in patients with liver IRE is to assess response to treatment, usually by evaluating residual contrast enhancement in post-operative images.

One of the first clinical studies on liver IRE that included MRI is a retrospective study of 28 patients with a total of 65 liver tumors [14]. Contrast-enhanced CT and/or MRI were acquired preoperatively to evaluate the size and location of tumors; IRE electrodes were placed with US or CT guidance to include a 1-cm margin around the tumor in the ablation zone. The imaging protocol was repeated in the immediate post-operative period, and 1, 3 and 6 months after treatment. One tumor had persistent disease, defined as residual contrast enhancement in the tumor area at the first follow-up imaging session, whereas in 3 cases there were local recurrences, defined as enhanced tumors within 1 cm of the ablation zone that were observed 2 to 8 months after IRE.

In a subsequent study, 44 patients (20 colorectal liver metastasis, 14 hepatocellular cancer, and 10 other metastases) undergoing IRE for hepatic tumors were evaluated [15]. Based on preoperative CT, tumor dimensions were measured and the treatment was planned. Post-operative CT or MRI were acquired shortly after the treatment and at 3-month intervals afterwards. Images were reviewed to identify the presence of residual viable tumor and the local recurrence-free survival rate was measured. The rate was 97.4% at 3 months, 94.6% at 6 months, and 59.5% at 12 months. Interestingly, when this analysis was repeated considering only lesions smaller than 3 cm, the local recurrence-free survival increased dramatically: 100% at 3 and 6 months and 98% at 12 months.

In a case report on a patient with hepatocellular carcinoma (HCC) adjacent to a transjugular

Table 1. Summary of liver IRE clinical studies including MRI acquisitions

Study	Primary aim	MRI sequences	Quantitative measures
Kingham et al., 2012 [14]	To evaluate recurrence and complications after liver IRE	Not specified	Tumor size Distance to the closest major hepatic vein or portal pedicle Area of the ablation zone
Mannelli et al., 2013 [17]	To report MRI appearance of a liver metastasis after IRE	Unenhanced and contrast-enhanced T1-weighted Diffusion-weighted (details not specified)	None
Cannon et al., 2013 [15]	To evaluate clinical safety and efficacy of IRE on hepatic tumors	Not specified	Tumor size
Niessen et al., 2013 [16]	To report IRE effects on a HCC lesion	T1-weighted Diffusion-weighted (details not specified)	None
Narayanan et al., 2014 [20]	To evaluate IRE effects on vessels in close proximity to the ablation zone	Contrast-enhanced (details not specified)	Distance from tumor to vessels
Granata et al., 2015 [13]	To report MRI findings after IRE of HCC	T2-weighted steady-state GRE T2-weighted FSE Diffusion-weighted T1-weighted GRE in 5 different phases after contrast administration (hepatic arterial, portal venous, equilibrium, delayed, hepatobiliary excretion)	Area of the ablation zone Apparent Diffusion Coefficient
Dollinger et al., 2015 [21]	To evaluate alterations in venous structures adjacent to the ablation zone after IRE of malignant hepatic tumors	Not specified	Tumor diameter Distance from IRE needle to closest vessel Vessel diameter
Granata et al., 2016 [18]	To compare the diagnostic accuracy of MRI, CT and US in the evaluation of the ablation area after IRE of HCC	T2-weighted steady-state GRE T2-weighted FSE Diffusion-weighted T1-weighted GRE in 5 different phases after contrast administration (hepatic arterial, portal venous, equilibrium, delayed, hepatobiliary excretion)	Tumor diameter Signal intensity Apparent Diffusion Coefficient
Padia et al., 2016 [19]	To assess MRI findings after IRE of HCC	T2-weighted TSE T1-weighted GRE pre-contrast and in 3 phases after contrast administration (hepatic arterial, portal venous and delayed)	Long and short axes of the ablation zone Periphery thickness Signal intensity
Dollinger et al., 2016 [22]	To evaluate biliary complications after IRE of malignant hepatic tumors	T1-weighted GRE acquired in the hepatobiliary phase after contrast administration	Bile duct diameter

Abbreviations: TSE = Turbo Spin Echo, GRE = Gradient Echo, FSE = Fast Spin Echo.

intrahepatic portosystemic shunt stent-graft [16], imaging was performed, including pre-operative contrast-enhanced US and MRI, intra-operative CT-fluoroscopy and US, post-operative contrast-enhanced US, CT and MRI 24 h and 8 weeks after IRE. Focusing on MRI, a T1-weighted sequence in the hepatobiliary phase and a diffusion-weighted sequence were acquired. In the pre-operative scans, the lesion was hypointense in T1-weighted and hyperintense on diffusion-weighted images. The post-operative scans showed a sharp demarcation of the hypointense ablation zone in the T1-weighted images and loss of the hyperintensity in the diffusion-weighted images, confirming the complete success of the ablation procedure.

In another case report on a liver metastasis [17], MRI was performed 1 day after IRE. A large area of ablation was evident at the site of the metastasis (**Figure 1A-C**), which presented no contrast enhancement and was thus presumed to be necrotic/apoptotic. It was surrounded by a rim of contrast enhancement (**Figure 1D**, **1E**) and hyperintensity in the diffusion-weighted images (**Figure 1F**). Images acquired 30 days later showed complete radiological liver parenchyma regeneration (**Figure 1G**).

Another group followed 20 patients undergoing IRE for HCC [13]. Contrast-enhanced US and MRI were acquired 5 days before and 1 month after IRE. The MRI acquisition protocol included T1-weighted, T2-weighted and diffusion-weighted imaging; in particular, dynamic T1-weighted images were acquired in 5 different phases: hepatic arterial, portal venous, equilibrium, delayed, and hepatobiliary excretion. At post-operative examination, 22 out of the 24 treated lesions showed complete response; the remaining two showed partial response, with areas of contrast enhancement during the arterial phase and portal phase washout. All the ablation zones appeared non-homogeneous hypoin-

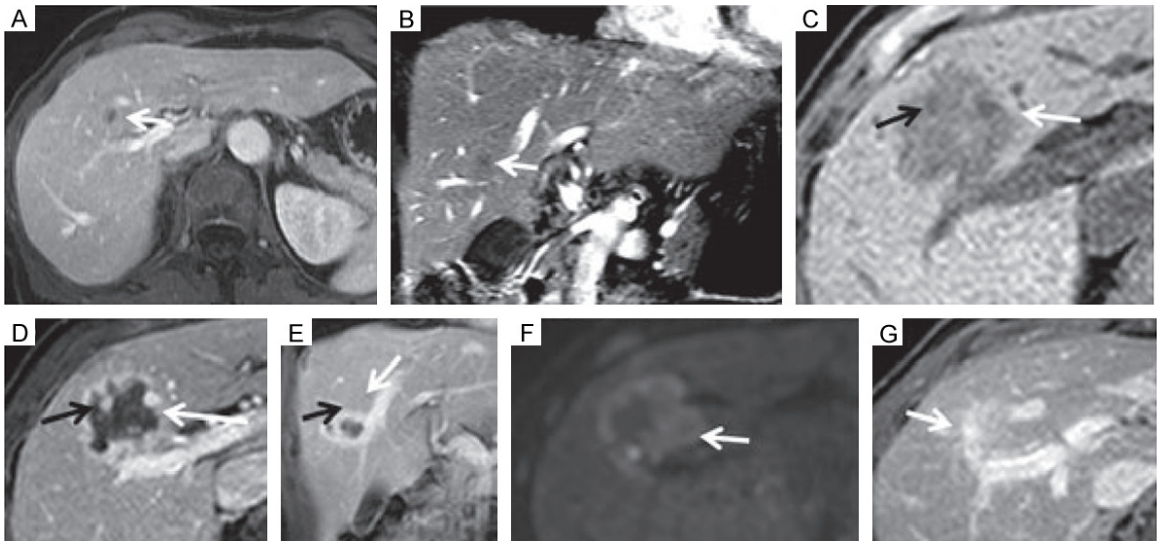

Figure 1. MRI appearance of a liver metastasis before and after IRE. (A, B) Pre-operative MRI showing the metastasis as an hypointense area. (C-E) Post-treatment MRI before (C) and after (D, E) contrast injection. (F) Post-treatment diffusion-weighted MRI. (G) Images acquired 30 days after IRE. Reproduced with permission from [17].

tense in the T2-weighted images and with a hyperintense central core surrounded by a hypointense rim in the T1-weighted images. The residual tumors appeared as hypointense areas in T1-weighted and hyperintense areas in T2-weighted images at the periphery of the ablation zones. The diffusion-weighted signal was hyperintense at b = 800 s/mm^2 in most of the cases, whereas in a few cases the lesions were not clearly visible at b = 0 s/mm^2 and the signal was not detectable at b = 800 s/mm^2. The size of the ablation areas was measured and it was 10% larger than at baseline imaging on average. Apparent diffusion coefficients were derived from diffusion-weighted images and measured in lesions. There was a trend towards higher diffusion coefficients one month after IRE with respect to baseline, although the difference was not statistically significant.

Data from the same patients were used to compare the diagnostic accuracy of contrast-enhanced US, CT and MRI 1, 3 and 6 months after IRE [18]. At the first time point, MRI and US showed complete response in 22 out of 24 lesions and progressive disease in the other two, with a residual tumor diameter of approximately 10 mm according to both modalities. On the other hand, all the treated areas appeared as necrotic on CT scans. At 3 months, MRI and US showed a very similar pattern compared to the scans at 1 month, with only a slight increase of the diameter of the two residual tumors measured using MRI (11 and 12 mm). CT showed 23 necrotic areas and one residual viable tumor with a diameter of 10 mm. At 6 months, all the three modalities showed 22 necrotic areas and 2 residual tumors, with diameters of 12 and 14 mm measured using MRI, 11 and 12 mm using US, and 10 and 10 mm using CT. The two residual tumors were treated again, and intra-operative US confirmed the lesion dimensions measured on MRI.

Finally, a recent retrospective study considered 20 patients with HCC [19]. The MRI protocol, including T2-weighted and dynamic contrast-enhanced T1-weighted sequences, was repeated 1 and 30 days after IRE, and every 90 days thereafter. At one month, 18 out of 20 patients had complete response to treatment and the other two had partial responses. One day after IRE, the ablated lesions showed a central area that was hyperintense in the T2-weighted and T1-weighted images, surrounded by a rim that was even more hyperintense in the T2-weighted images, hypointense on the unenhanced T1-weighted images and hyperintense in the enhanced T1-weighted images (**Figure 2D-F**). The size of the ablation zone and the periphery decreased over time, with the largest decrease occurring in the first 30 days. The T2-weighted signal tended to decrease over time. The T1-weighted signal in the tumor tended to increase and the signal in the periphery tended to increase in unenhanced and decrease in

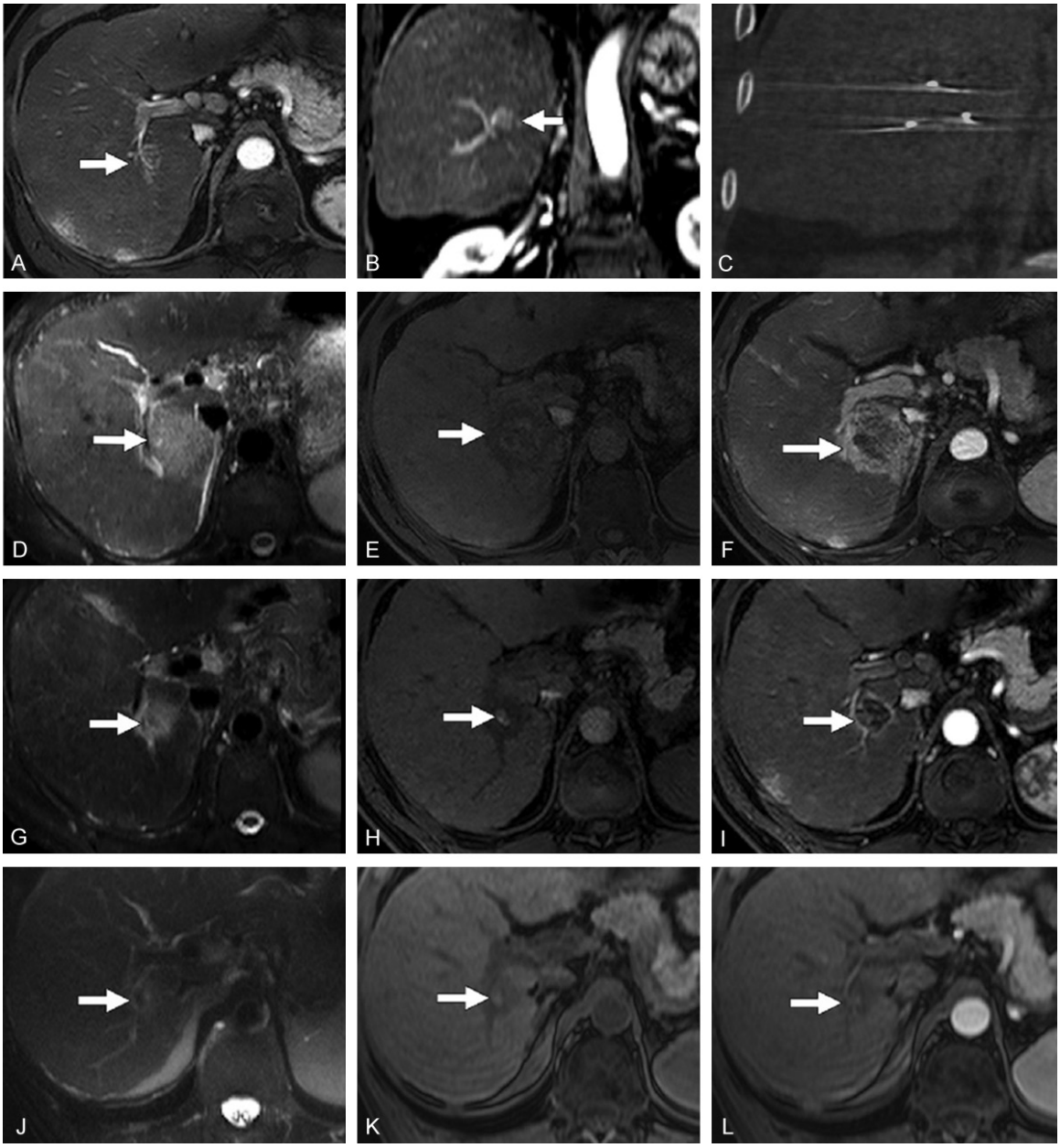

Figure 2. Typical MRI appearance of HCC after IRE. (A, B) Baseline axial and coronal contrast-enhance T1-weighted MRI acquired in the arterial phase showing an HCC in the right hepatic lobe. (C) Post-IRE CT showing the electrodes. (D-F) Images acquired 24 hours after IRE, showing an ablation area that is hyperintense at T2-weighted MRI (D), slightly hyperintense with an hypointense margin at unenhanced T1-weighted MRI (E) and hypointense with hyperintense margin at contrast-enhanced T1-weighted MRI during the arterial phase (F). (G-I) T2-weighted MRI (G), unenhanced (H) and contrast-enhanced (I) T1-weighted MRI acquired 30 days after IRE, showing similar signals but reduced dimensions with respect to the previous time point. (J-L) T2-weighted MRI (J), unenhanced (K) and contrast-enhanced (L) T1-weighted MRI acquired 120 days after IRE, showing a further reduction of the ablation zone and no contrast enhancement. Reproduced with permission from [19].

enhanced T1-weighted images (**Figure 2G-L**). The authors speculated that the peripheral enhancing zone, resolving over time, could be a penumbra of reversible electroporation.

Assessment of complications after IRE

Another important aim of post-operative MRI in liver IRE clinical studies is the assessment of

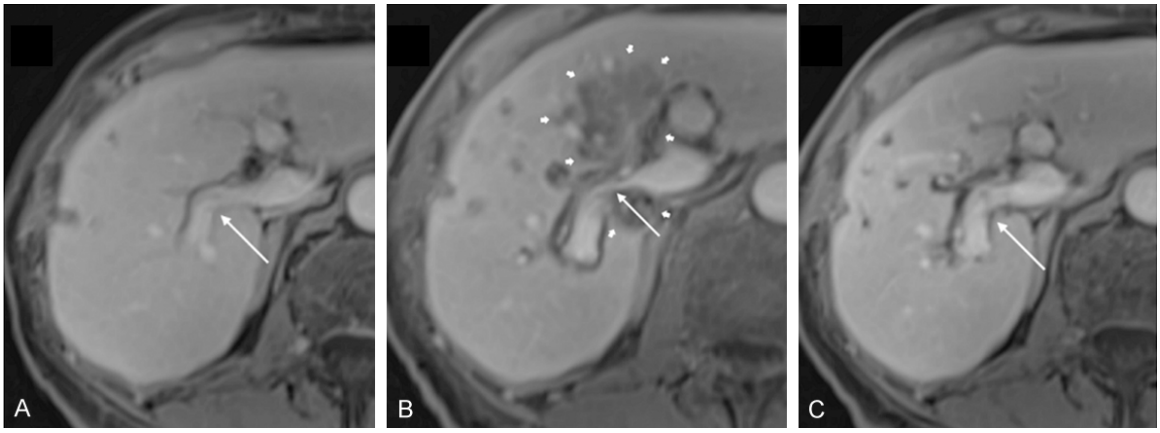

Figure 3. Portal vein narrowing in a case of colorectal cancer. A: Pre-interventional contrast-enhanced T1-weighted MRI shows a freely perfused right branch of the portal vein (thin arrow). B: 3 days after IRE, MRI shows a caliber reduction of the right portal vein (thin arrow), encased by the ablation zone (thick arrows). C: 6 weeks after treatment, the lumen reduction of the right portal vein (thin arrow) has resolved. Reproduced from [21].

complications occurring to surrounding structures after treatment.

In the study by Kingham et al. cited in the previous section [14], post-operative images were also reviewed to assess complications involving vessels included in the ablation zone. Major hepatic veins and portal pedicles were within 1 cm from tumors in 57% and 40% of the cases, respectively. All the structures were patent at follow-up imaging, with the only exception being one portal pedicle, in which post-operative imaging showed a thrombus.

More recently, Narayanan et al. [20] examined 101 patients undergoing percutaneous IRE procedures for 129 lesions in different organs, with the great majority (78%) in the liver. Contrast-enhanced CT or MRI was acquired 1, 3, 6 and 12 months after treatment to evaluate caliber, patency, and flow defects of vessels in close proximity (within 1 cm) to the ablation zone. One hundred fifty-eight of these vessels were identified, including 40 abutting and 10 encased by the tumor. Abnormal vascular changes were only found in 7 cases, including 4 thromboses of the portal veins and 3 cases of mild narrowing. No significant association was found between the presence of narrowing/thrombosis at follow-up imaging and the distance from the treatment zone.

A similar study examined 43 patients with venous structures within 1 cm from the ablation zone after IRE of 84 hepatic lesions [21]. Contrast-enhanced CT or MRI was acquired during the portal venous phase before and after each intervention. Fifty-five venous structures were found to be surrounded by the ablation zone, 78 abutting the ablation zone and 58 between 0.1 and 1 cm away from the ablation zone, for a total of 191 examined vessels. Follow-up imaging was performed 1 to 3 days after treatment and showed abnormal changes in 19 vessels, including 5 portal vein thromboses and 14 cases of lumen narrowing (**Figure 3**). Patients with subacute alterations were followed by further follow-up imaging (6 ± 4 months later). Two out of the 5 thromboses resolved, 8 out of the 14 cases with vessel narrowing also completely resolved and another one partly resolved. In this study, significant associations were found between post-IRE vessel alterations and the encasement of a vessel by the ablation zone, with the ablation zone being adjacent to a portal vein, or the usage of more than 3 IRE probes.

The same group examined 24 patients with bile ducts within 1 cm from the ablation zone after percutaneous IRE of 53 hepatic tumors [22]. Pre- and post-interventional T1-weighted MRI was acquired 20 minutes after the injection of hepatocyte-specific Gd contrast (during the hepatobiliary phase). Thirty-three bile ducts were found to be encased, 14 abutting and 8 within a radius of 0.1-1.0 cm of the ablation zone, for a total of 55 bile ducts examined for changes in caliber, patency, and leakage. MRI was performed 1-3 days after IRE, and it

Table 2. Summary of liver IRE preclinical studies including MRI acquisitions

Study	Primary aim	MRI sequences	Quantitative measures
Guo et al., 2010 [25]	To observe tumor evolution after IRE	T2-weighted TSE T1-weighted TSE PD-weighted TSE	Maximum lesion diameter Lesion cross-sectional area
Lee et al., 2010 [10]	To evaluate IRE effects on the healthy liver and their appearance at MRI	T1-weighted GRE (before contrast administration and in the hepatic arterial and portal venous phases)	None
Zhang et al., 2010 [23]	To test the possibility to detect IRE effects by MRI immediately after treatment of the healthy liver	T1-weighted GRE T2-weighted TSE T1-weighted TSE PD-weighted TSE	Area of the ablation zone
Guo et al., 2011 [24]	To evaluate ablation zones measures in the healthy liver by different MRI sequences	T1-weighted GRE IR FLASH with multiple inversion times	Area of the IRE ablation zone Area of the RE penumbra
Zhang et al., 2014 [26]	To compare alterations shown by different imaging modalities after IRE in liver tumors	T1-weighted GRE T2-weighted FSE	Signal-to-noise Ratio before and after IRE

Abbreviations: TSE = Turbo Spin Echo, PD = Proton Density, GRE = Gradient Echo, IR = Inversion Recovery, FLASH = Fast Low Angle Shot, FSE = Fast Spin Echo.

showed 15 alterations, including dilations in 3 encased, 3 abutting and one distant bile ducts, and the narrowing of 8 encased bile ducts. These patients were followed by further follow-up imaging (7.2 ± 5.3 months later); only the 3 cases of dilated bile ducts encased by the ablation zone persisted at this time.

Preclinical studies

Preclinical studies have a different approach with respect to clinical ones: here the interest is not only in the success of the ablation procedure but also in understanding the biological events occurring in the treated area over time and how they can be monitored by imaging techniques. More attention is paid to the choice of acquisition protocol and to the attainment of quantitative measures (**Table 2**), validated by either histology or other techniques.

The difference with respect to clinical studies is also reflected in the type of target tissues in preclinical IRE studies. In preclinical animal studies, there is always an untreated group and often animals with no tumors are included; IRE can be performed also on the healthy liver to understand its effects, size of ablation zone, and how tissue alterations appear in images acquired with different modalities. These changes and their imaging manifestation are discussed below.

Studies on the healthy liver

The earliest preclinical study on IRE of the healthy liver with MRI scans included 16 pigs [10]. A total of 55 ablation zones were produced. The main imaging modality in this work was US, which was acquired during and immediately after the procedure, and again the next day. Two days after IRE, 2 animals with 6 ablation zones were imaged by CT and 2 different animals with 6 ablation zones were imaged by MRI. The MRI protocol included a dynamic contrast-enhanced T1-weighted sequence. The ablation zones appeared as hypointense on T1-weighted images, with a mildly enhancing rim. This work demonstrated that ablation areas can be monitored by real-time US and reliably assessed by contrast-enhanced CT or MRI.

In another study [23], 18 healthy rats were divided into 3 groups undergoing liver IRE with different voltages (1000, 1500 and 2500 V). Proton density, T1- and T2-weighted MRI sequences were acquired before and immediately after the treatment. Ablation areas appeared as hyperintense on T2-weighted and hypointense on T1-weighted images compared to pre-operative images. Regions of interest were manually delineated in these ablation zones and their area was measured. The results were compared with the areas anticipated by

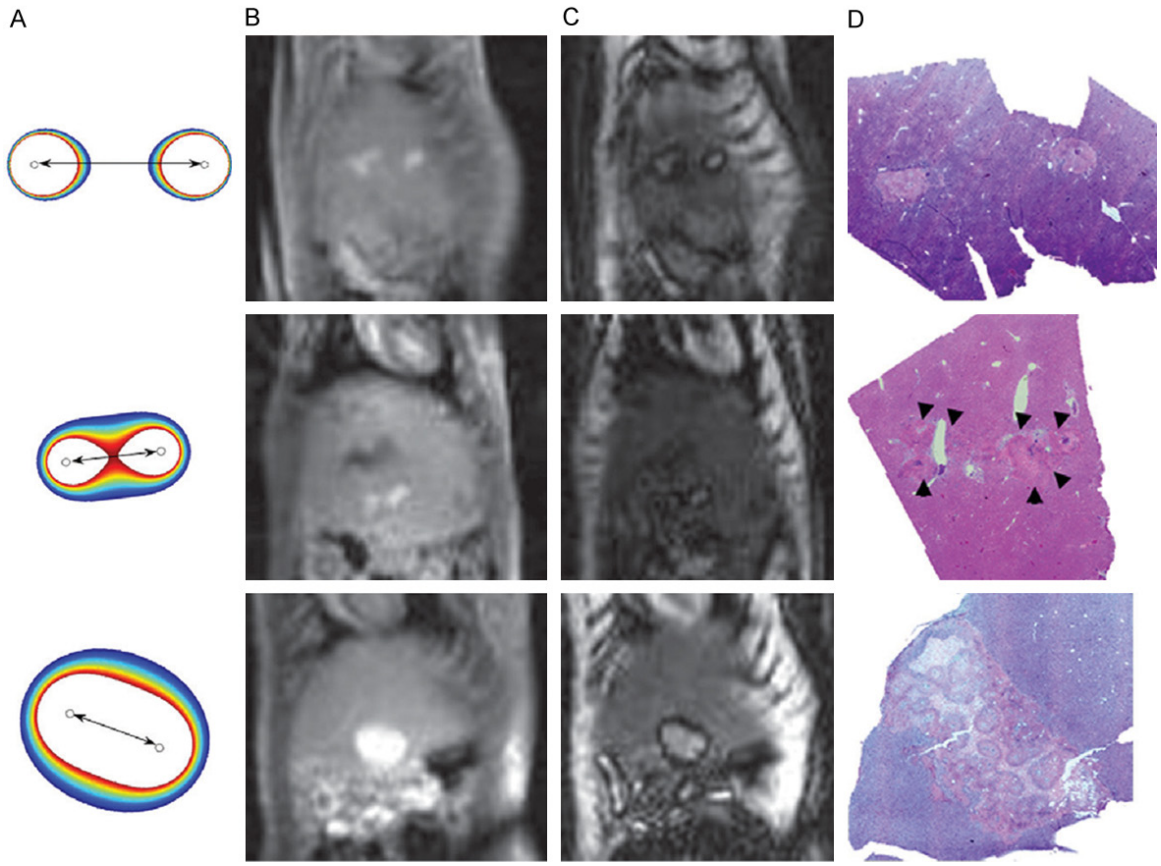

Figure 4. IRE effects on the healthy liver in rats. A: Finite-element modeling simulations showing the anticipated IRE zone (white area) and RE penumbra (colored zones) corresponding to the 3 different electrodes configurations. B: Post-IRE T1-weighted gradient-echo MRI. C: Post-IRE inversion recovery MRI adjusted to null the signal in the RE penumbra. D: Corresponding hematoxylin-eosin-stained histology slices. Reproduced with permission from [24].

finite element modeling and with those measured on histologic slides stained with hematoxylin-eosin. The 3 sets of measures showed a very good correlation, with larger areas for higher voltage.

Finally, Guo et al. [24] performed liver IRE in 17 healthy rats. The animals were divided into 4 groups: 3 underwent IRE with different parameters (voltage and electrode spacing) after the injection of a contrast agent, whereas the fourth had IRE and MRI with no injected contrast. The MRI acquisition protocol included a T1-weighted gradient-echo sequence and an inversion recovery (IR) sequence with different inversion times that were expected to null the signal in the normal liver, in the ablation area or in the surrounding penumbra (area of reversible electroporation). Lesions were uniformly hyperintense in the gradient-echo images and in the IR images with the inversion time nulling the signal in the normal liver. On IR images with the inversion time expected to null the signal in the penumbra, a central hyperintense lesion was surrounded by a hypointense periphery (**Figure 4**). Using the different acquired images as visual references, regions of interest were drawn on areas of irreversible and reversible electroporation. The areas measured on all the sequences were well correlated with those derived from hematoxylin-eosin histology, with highest correlation provided by the penumbra-nulling IR sequence, whereas the gradient-echo and the normal liver-nulling IR sequences tended to overestimate the ablation area compared to histology.

Studies on liver tumors

The earliest MRI study of IRE in an animal model of liver tumors included 30 rats with HCC that were divided into 4 treated and 2 control groups with different sacrifice times [25]. The MRI protocol included proton density,

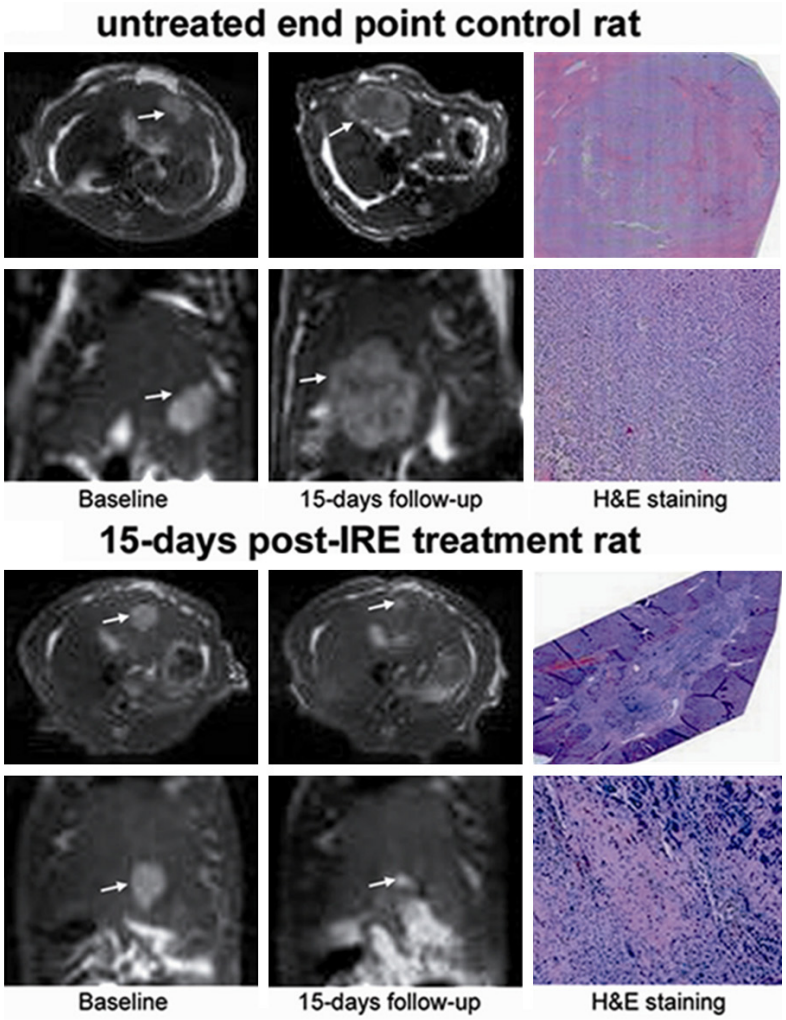

Figure 5. Comparison of MRI and histology in rats with HCC, untreated or treated with IRE. Top panel: untreated rat; bottom panel: IRE-treated rat. Left: axial and coronal baseline T2-weighted images, acquired shortly before IRE for the treated rats. Center: axial and coronal T2-weighted images acquired 15 days later. Right: corresponding ematoxylin-eosin-stained histology slides. Reproduced with permission from [25].

T1-weighted and T2-weighted sequences and was performed at baseline and before euthanizing each animal. Tumors appeared as consistently hyperintense in the T2-weighted images, hypointense in the T1-weighted images and typically isointense in the proton density images (**Figure 5**). The size of the lesions was measured as the maximum diameter and the cross-sectional area. Both measures decreased in the treated tumors (-32% and -52% on average, respectively) and considerably increased in all the untreated tumors (+110% and +286% on average, respectively).

In another study [26] 48 rats were divided into 8 groups according to the type of tissue considered (healthy or tumor), the procedure that was conducted (IRE, IRE with vessel ligation or no treatment) and the imaging modality used to follow them (US, CT or MRI). The MRI protocol included a T1-weighted and a T2-weighted sequence with no injection of contrast agent. The normal liver tissue and the tumor were hypointense in the T1-weighted and hyperintense in the T2-weighted images after IRE. The signal-to-noise ratio in the normal liver decreased significantly after IRE on T1-weighted images and increased significantly on T2-weighted images, whereas in tumors no significant change was observed following IRE. The tumors treated after hepatic vessel ligation showed no MRI signal change after IRE, suggesting that early signal changes are likely the result of local fluid accumulation owing to transient permeabilization of blood vessels, with subsequent fluid build-up after rapid extravasation into the treated tissue zones.

Conclusion and future perspectives

MRI is still not the primary choice for imaging in liver IRE studies. However, the interesting preliminary results provided by several studies and the potential superiority in assessment of tumor response to IRE compared to other imaging techniques should foster a wider application of MRI. The feasibility and utility of advanced and quantitative techniques such as diffusion and perfusion MRI which are sensitive to microstructural and vascular alteration remain to be fully studied. This could improve the understanding of the biophysical processes involved in the tissue response to IRE and may provide functional biomarkers of treatment efficacy that are more reliable than T1-weighted, T2-weighted, and contrast enhanced MRI approaches.

Acknowledgements

This work was supported by the USA National Cancer Institute R01CA209886-01 and R01-CA196967.

Disclosure of conflict of interest

None.

Address correspondence to: Zhuoli Zhang, Department of Radiology, Robert H. Lurie Comprehensive Cancer Center, Northwestern University, 737 N. Michigan Ave, 16th Floor, Chicago, IL 60611, USA. Tel: 312-926-3874; Fax: 312-926-5991; E-mail: zhuoli-zhang@northwestern.edu

References

[1] Davalos RV, Mir IL and Rubinsky B. Tissue ablation with irreversible electroporation. Ann Biomed Eng 2005; 33: 223-231.

[2] Scheffer HJ, Nielsen K, de Jong MC, van Tilborg AA, Vieveen JM, Bouwman AR, Meijer S, van Kuijk C, van den Tol PM and Meijerink MR. Irreversible electroporation for nonthermal tumor ablation in the clinical setting: a systematic review of safety and efficacy. J Vasc Interv Radiol 2014; 25: 997-1011; quiz 1011.

[3] Valerio M, Stricker PD, Ahmed HU, Dickinson L, Ponsky L, Shnier R, Allen C and Emberton M. Initial assessment of safety and clinical feasibility of irreversible electroporation in the focal treatment of prostate cancer. Prostate Cancer Prostatic Dis 2014; 17: 343-347.

[4] Paiella S, Butturini G, Frigerio I, Salvia R, Armatura G, Bacchion M, Fontana M, D'Onofrio M, Martone E and Bassi C. Safety and feasibility of Irreversible Electroporation (IRE) in patients with locally advanced pancreatic cancer: results of a prospective study. Dig Surg 2015; 32: 90-97.

[5] Rossmeisl JH Jr, Garcia PA, Pancotto TE, Robertson JL, Henao-Guerrero N, Neal RE 2nd, Ellis TL and Davalos RV. Safety and feasibility of the NanoKnife system for irreversible electroporation ablative treatment of canine spontaneous intracranial gliomas. J Neurosurg 2015; 123: 1008-1025.

[6] Wagstaff PG, de Bruin DM, Zondervan PJ, Savci Heijink CD, Engelbrecht MR, van Delden OM, van Leeuwen TG, Wijkstra H, de la Rosette JJ and Laguna Pes MP. The efficacy and safety of irreversible electroporation for the ablation of renal masses: a prospective, human, in-vivo study protocol. BMC Cancer 2015; 15: 165.

[7] Chen X, Ren Z, Zhu T, Zhang X, Peng Z, Xie H, Zhou L, Yin S, Sun J and Zheng S. Electric Ablation with Irreversible Electroporation (IRE) in Vital Hepatic Structures and Follow-up Investigation. Sci Rep 2015; 5: 16233.

[8] Lee EW, Thai S and Kee ST. Irreversible electroporation: a novel image-guided cancer therapy. Gut Liver 2010; 4 Suppl 1: S99-s104.

[9] Savic LJ, Chapiro J, Hamm B, Gebauer B and Collettini F. Irreversible Electroporation in Interventional Oncology: Where We Stand and Where We Go. Rofo 2016; 188: 735-745.

[10] Lee EW, Chen C, Prieto VE, Dry SM, Loh CT and Kee ST. Advanced hepatic ablation technique for creating complete cell death: irreversible electroporation. Radiology 2010; 255: 426-433.

[11] Charpentier KP, Wolf F, Noble L, Winn B, Resnick M and Dupuy DE. Irreversible electroporation of the liver and liver hilum in swine. HPB (Oxford) 2011; 13: 168-173.

[12] Lee YJ, Lu DS, Osuagwu F and Lassman C. Irreversible electroporation in porcine liver: short- and long-term effect on the hepatic veins and adjacent tissue by CT with pathological correlation. Invest Radiol 2012; 47: 671-675.

[13] Granata V, Fusco R, Catalano O, Piccirillo M, De Bellis M, Izzo F and Petrillo A. Percutaneous ablation therapy of hepatocellular carcinoma with irreversible electroporation: MRI findings. AJR Am J Roentgenol 2015; 204: 1000-1007.

[14] Kingham TP, Karkar AM, D'Angelica MI, Allen PJ, Dematteo RP, Getrajdman GI, Sofocleous CT, Solomon SB, Jarnagin WR and Fong Y. Ablation of perivascular hepatic malignant tumors with irreversible electroporation. J Am Coll Surg 2012; 215: 379-387.

[15] Cannon R, Ellis S, Hayes D, Narayanan G and Martin RC 2nd. Safety and early efficacy of irreversible electroporation for hepatic tumors in proximity to vital structures. J Surg Oncol 2013; 107: 544-549.

[16] Niessen C, Jung EM, Wohlgemuth WA, Trabold B, Haimerl M, Schreyer A, Stroszczynski C and Wiggermann P. Irreversible electroporation of a hepatocellular carcinoma lesion adjacent to a transjugular intrahepatic portosystemic shunt stent graft. Korean J Radiol 2013; 14: 797-800.

[17] Mannelli L, Padia SA, Yeung RS and Green DE. Irreversible electroporation of a liver metastasis. Liver Int 2013; 33: 104.

[18] Granata V, de Lutio di Castelguidone E, Fusco R, Catalano O, Piccirillo M, Palaia R, Izzo F, Gallipoli AD and Petrillo A. Irreversible electroporation of hepatocellular carcinoma: preliminary report on the diagnostic accuracy of magnetic resonance, computer tomography, and contrast-enhanced ultrasound in evaluation of the ablated area. Radiol Med 2016; 121: 122-131.

[19] Padia SA, Johnson GE, Yeung RS, Park JO, Hippe DS and Kogut MJ. Irreversible Electroporation in Patients with Hepatocellular Carcinoma: Immediate versus Delayed Findings at MR Imaging. Radiology 2016; 278: 285-294.
[20] Narayanan G, Bhatia S, Echenique A, Suthar R, Barbery K and Yrizarry J. Vessel patency post irreversible electroporation. Cardiovasc Intervent Radiol 2014; 37: 1523-1529.
[21] Dollinger M, Muller-Wille R, Zeman F, Haimerl M, Niessen C, Beyer LP, Lang SA, Teufel A, Stroszczynski C and Wiggermann P. Irreversible Electroporation of Malignant Hepatic Tumors--Alterations in Venous Structures at Subacute Follow-Up and Evolution at Mid-Term Follow-Up. PLoS One 2015; 10: e0135773.
[22] Dollinger M, Zeman F, Niessen C, Lang SA, Beyer LP, Muller M, Stroszczynski C and Wiggermann P. Bile Duct Injury after Irreversible Electroporation of Hepatic Malignancies: Evaluation of MR Imaging Findings and Laboratory Values. J Vasc Interv Radiol 2016; 27: 96-103.
[23] Zhang Y, Guo Y, Ragin AB, Lewandowski RJ, Yang GY, Nijm GM, Sahakian AV, Omary RA and Larson AC. MR imaging to assess immediate response to irreversible electroporation for targeted ablation of liver tissues: preclinical feasibility studies in a rodent model. Radiology 2010; 256: 424-432.
[24] Guo Y, Zhang Y, Nijm GM, Sahakian AV, Yang GY, Omary RA and Larson AC. Irreversible electroporation in the liver: contrast-enhanced inversion-recovery MR imaging approaches to differentiate reversibly electroporated penumbra from irreversibly electroporated ablation zones. Radiology 2011; 258: 461-468.
[25] Guo Y, Zhang Y, Klein R, Nijm GM, Sahakian AV, Omary RA, Yang GY and Larson AC. Irreversible electroporation therapy in the liver: longitudinal efficacy studies in a rat model of hepatocellular carcinoma. Cancer Res 2010; 70: 1555-1563.
[26] Zhang Y, White SB, Nicolai JR, Zhang Z, West DL, Kim DH, Goodwin AL, Miller FH, Omary RA and Larson AC. Multimodality imaging to assess immediate response to irreversible electroporation in a rat liver tumor model. Radiology 2014; 271: 721-729.